Earthquakes and Structures, *Vol. 6, No. 3 (2014) 251-266*
DOI: http://dx.doi.org/10.12989/eas.2014.6.3.251

Earthquake stresses and effective damping in concrete gravity dams

Uğur Akpınar, Barış Binici* and Yalın Arıcı

Department of Civil Engineering, Middle East Technical University, Ankara, Turkey

(Received July 31, 2013, Revised November 22, 2013, Accepted December 9, 2013)

Abstract. Dynamic analyses for a suite of ground of motions were conducted on concrete gravity dam sections to examine the earthquake induced stresses and effective damping. For this purpose, frequency domain methods that rigorously incorporate dam-reservoir-foundation interaction and time domain methods with approximate hydrodynamic foundation interaction effects were employed. The maximum principal tensile stresses and their distribution at the dam base, which are important parameters for concrete dam design, were obtained using the frequency domain approach. Prediction equations were proposed for these stresses and their distribution at the dam base. Comparisons of the stress results obtained using frequency and time domain methods revealed that the dam height and ratio of modulus of elasticity of foundation rock to concrete are significant parameters that may influence earthquake induced stresses. A new effective damping prediction equation was proposed in order to estimate earthquake stresses accurately with the approximate time domain approach.

Keywords: concrete gravity dams; stress estimation; damping; numerical simulation; linear dynamic analysis; dam-reservoir-foundation interaction

1. Introduction

The potential of hydropower was utilized efficiently by the end of 1980s in most of the developed nations. However, dams are still under construction in countries with emerging economies such as Turkey and China. For example, the number of dams constructed in Turkey since 1930's up to 2006 is about 600 whereas about 200 new dams are currently under planning, design or construction stage. In this context, roller compacted concrete (RCC) dams are widely preferred, especially if fly ash and/or pozzolans are available at the dam site, due to their advantages such as possibility of rapid construction, better control of heat generation of concrete and the economy. Such benefits of RCC make them the leading candidate material in the dam design. For preliminary dam design and surveying the existing dam stock, conducting rigid block stability analysis may be considered as a first stage approach. However, if the foundation rock properties along with the expected strong motions are to be considered, dynamic analyses play a critical role in seismic design of new concrete dams and evaluation of existing concrete dams.

The pioneering work of Westergaard (1933) provided means of estimating hydrodynamic pressure on rigid dams during earthquakes. The next milestone on the topic was calculation of

*Corresponding author, Professor, E-mail: binici@metu.edu.tr

http://www.techno-press.org/?journal=eas&subpage=7 ISSN: 2092-7614 (Print), 2092-7622 (Online)

earthquake response of rigid dams considering the compressibility effect of the water by Chopra (1966). Afterwards, studies focused on numerical investigation of dam-reservoir and dam-foundation interactions making use of the finite element method. The works of Fenves and Chopra (1984-1986) on a combined numerical-analytical technique provided means of accurate stress estimations. Their technique rigorously handled the radiation damping due to infinite reservoir and half-space foundation flexibility with a substructure approach in the frequency domain. Lotfi *et al*. (1987), on the other hand, considered the foundation (as a deep stratum) and reservoir with consistent transmitting hyper-elements. The hyper-element technique presented by Lotfi *et al.* (1987) and the boundary element approach of Dominguez *et al.* (1990) included water-sediment interaction, where both studies employed the work of Fenves and Chopra (1984) as the benchmark. Bougacha and Tassoulas (1993) did further work on the effect of sediments by considering the sediments as a porous medium for a better understanding of their importance in the seismic response. All of the above studies were conducted in the frequency domain thereby permitting the evaluation of the dynamic response of dam sections by incorporating two important effects: 1) waves carrying energy from the foundation in the proximity of the dam to infinity, appearing as an effective damping, 2) the compressibility of the water and ensuring that wave reflections at boundaries are eliminated at infinite reservoir boundaries.

Nowadays, the need of estimating the potential risks and expected loss under earthquakes has shifted the engineers to conduct nonlinear analysis of structures including dams. A number of studies were conducted to investigate concrete cracking and estimate dam stability (e.g., Bhattacharjee *et al.* 1995, Mclean *et al.* 2006 and Arici *et al.* 2011). In such nonlinear analysis, most practicing engineers still use the massless foundation and added mass hydrodynamic models to simulate the dam-reservoir-foundation interaction due to their advantages such as allowing the use of existing software and providing computational efficiency while analyzing many alternative sections with many load cases (e.g., Javanmardi *et al.* 2005 and Lotfi *et al.* 2008). The most important prerequisite of such analyses is the selection of the effective damping, for which the seismic response and stresses can be estimated close to those obtained by using rigorous frequency domain approaches.

The objective of this study is two folds: First, earthquake induced dam stresses are examined for typical dam sections with various heights and material properties by using the combined analytical-numerical technique of Fenves and Chopra (1984). Afterwards, prediction equations are developed to estimate the maximum principal tensile stress demand and their distribution along the dam base. The proposed equations can be employed in the preliminary design or seismic assessment of gravity dams. Secondly, the stress errors upon using massless foundation models with added mass approach along with the apparent damping as proposed by Fenves and Chopra (1986) are critically evaluated. A new equation for the effective damping is proposed for use in response history analysis in the time domain for accurate stress estimations. The outcomes of this study are believed to help practicing engineers in realizing and considering the importance of dam-reservoir-foundation interactions.

2. "EXACT" earthquake dam stresses

2.1 Analysis procedure and cases

The literature review given above revealed that procedure of Fenves and Chopra (1984) is still the state of the art for the linear elastic response history analysis of gravity dams. Therefore, this procedure, named as the "Exact Model, EM" (Fig. 1(a)), was accepted as the exact solution for the seismic response history analysis. The technique of Fenves and Chopra (1984) is a frequency domain hybrid numerical and analytical finite element approach. In their substructure approach, the equation of motion of the dam-reservoir-foundation system is solved for each excitation frequency by employing the reduced degrees of freedom obtained from the Ritz procedure. EM utilizes exact solution of hydrodynamic forces of an infinite channel on the upstream face of the dam and it includes the two-dimensional half space flexible foundation response under seismic excitations. In the formulation, the complex valued foundation stiffness matrix was obtained by using the numerical method proposed by Dasgupta and Chopra (1977). The bottom absorption is approximately modeled by the modification of the boundary condition at the reservoir bottom. Its effect is included by a wave reflection coefficient (α) that represents the ratio of the amplitude of reflected hydrodynamic pressure wave to the amplitude of a vertically propagating pressure wave incident on the reservoir bottom, which depends on damping coefficient of the reservoir materials, and velocity of pressure waves in water.

The flexible foundation solution of the original program (EAGD84) prepared by Fenves and Chopra (1984) supplies the dynamic stiffness influence coefficients for a foundation mesh of only 8 elements with only constant values of foundation damping (for 2%, 5% and 10% damping ratios). In order to overcome these restrictions, a new program to compute the foundation compliances for models with denser meshes and arbitrary foundation damping values was prepared. The influence coefficients were recalculated using the procedures of Dasgupta and Chopra (1977). In addition, a standalone user friendly pre and post processor was prepared.

A number of dam sections representative of almost all practical cases were analyzed using the EM. The dam heights (H) were chosen as 50, 100, 150 m. Upstream face of all dam sections were vertical and the corresponding downstream slopes (S) were selected as 0.8 and 1.0. Crest length of the dams were taken as 4 m, 8 m and 12 m for the dam heights of 50, 100, and 150 m, respectively. Dam sections were analyzed both for the empty and full reservoir conditions to reflect the two extreme conditions. Modulus of elasticity of concrete (E_c) for dam body was taken as 20000 MPa and 30000 MPa. Modulus of elasticity of the foundation rock (E_f) was included in the analysis as a fraction of concrete modulus of elasticity (i.e E_f/E_c= 0.5, 1, 2, 10, 50). It was identified that a

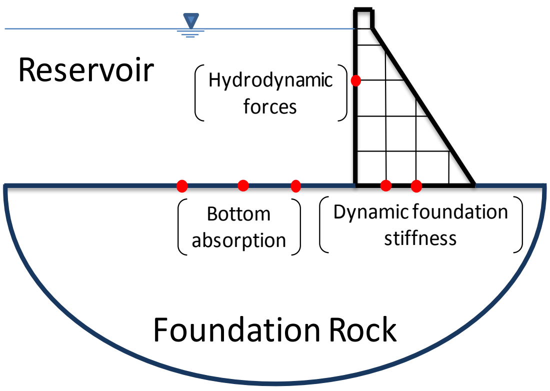

(a) EM: "Exact" approach

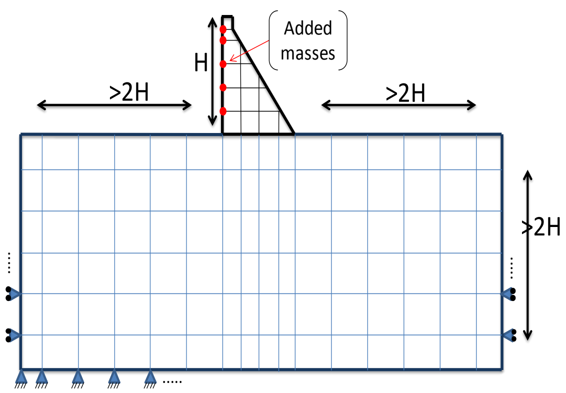

(b) IFMFM: "Simplified" approach

Fig. 1 Demonstration of EM and IFMFM

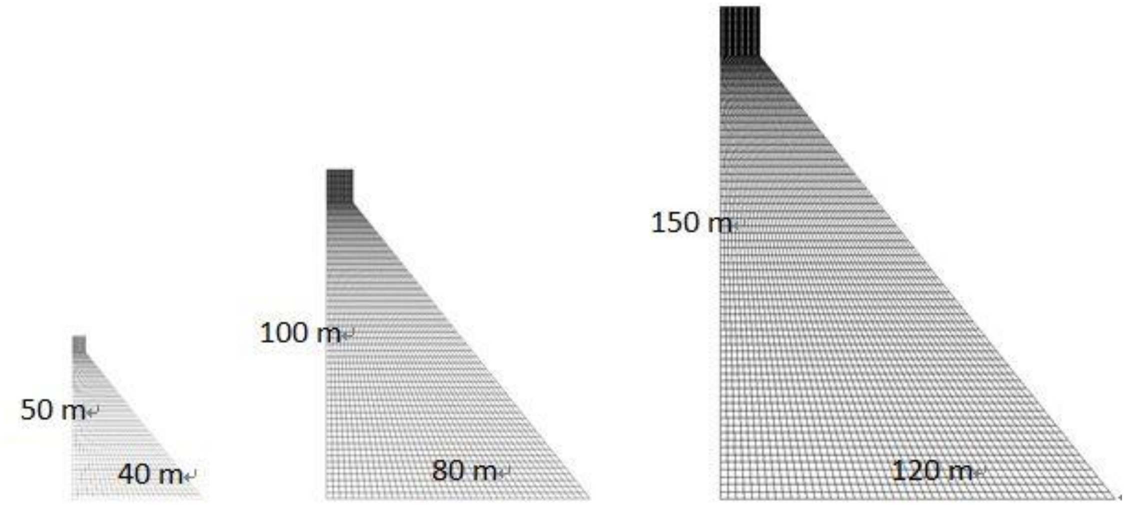

(a) Section 1 (b) Section 2 (c) Section 3

Fig. 2 Finite element meshes for analyzed cases

flexible base solution with an E_f/E_c = 50 ratio practically corresponds to a fixed base dam without any structure-foundation interaction. Along with the employed parameters, 120 different dam models were used.

For all cases, the densities of concrete and foundation rock material were taken as 2400 kg/m^3. Poisson's ratios of concrete and foundation rock were assumed as 0.2 and 0.25, respectively. In order to follow the common practice, a 5% hysteretic damping ratio for the concrete and foundation rock was used in all analyses with EM. Wave reflection coefficient was assumed to be one in all analysis to reflect the insignificant sedimentation in new dams. Finite element meshes used in the analyses are presented in Fig. 2. The number of elements was proportionally increased to keep element sizes constant for the examined dam sections. A further mesh refinement study was conducted by using a mesh with twice the number of elements along the base compared to those shown in Fig. 2. For the maximum principal stress, error was less than 1% at the examined location for the chosen mesh. Upon consideration of the computational cost, the selected mesh density was deemed satisfactory for the purposes of this investigation.

2.2 Ground motions

Thirty-seven different ground motion records were utilized for the dynamic analyses of each dam section. Ground motions were selected such that shear wave velocity of the recorded motion location was greater than 750 m/s to realistically represent the foundation rock properties of concrete dam sites. The complete list of ground motion records are given in Table 1.

The ranges of interest for M_w (moment magnitude), d (distance to epicenter), PGA (peak ground acceleration) and PGV (peak ground velocity) are as follows: 5.7 < M_w < 7.4, 4 km < d < 78 km, 0.024 g < PGA < 1.497 g, 1.90 cm/s < PGV < 126.12 cm/s. M_L, d_c and d_h represent the local magnitude, closest distance and hypocentral distance, respectively. The response spectra of the ground motions are presented in Fig. 3 for all motion records. The selected parameters (i.e.,

Table 1 Details of ground motion records

Earthquake	Country	Date	Site Geo.	Comp.	d (km)	M_w	PGA(g)	PGV(cm/s)
Vrancea	Romania	1990	Rock	EW	5	6.6(M_L)	0.024	1.90
Vrancea	Romania	1990	Rock	NS	5	6.6(M_L)	0.030	2.18
Marmara	Turkey	1999	Rock	NS	78	7.4	0.052	4.30
Loma Prieta	USA	1989	NEHRP(B)	115	53(d_c)	7	0.058	6.13
Loma Prieta	USA	1989	NEHRP(B)	205	53(d_c)	7	0.105	8.19
Marmara	Turkey	1999	Rock	EW	78	7.4	0.106	14.92
Imperial Valley	USA	1979	Granite	N45E	21.8(d_c)	6.5	0.110	5.14
Lazio Abruzzo	Italy	1984	Rock	EW	60	5.7	0.126	7.30
Lazio Abruzzo	Italy	1984	Rock	NS	60	5.7	0.132	9.47
Northridge	USA	1994	Rock	90	36.7(d_c)	6.7	0.133	5.34
Coalinga	USA	1983	Granite	315	35(d_h)	6.5	0.136	15.62
Campano-Luc.	Italy	1980	Rock	NS	23	6.5	0.139	20.57
Bucharest	Romania	1977	Rock	EW	4	6.4(M_L)	0.151	25.64
Marmara	Turkey	1999	Rock	NS	11	7.4	0.167	32.04
Coalinga	USA	1983	Granite	45	35(d_h)	6.5	0.172	15.75
Campano-Luc.	Italy	1980	Rock	EW	23	6.5	0.181	30.45
Imperial Valley	USA	1979	Granite	S45E	21.8(d_c)	6.5	0.186	8.65
Bucharest	Romania	1977	Rock	NS	4	6.4(M_L)	0.194	70.55
Campano-Luc.	Italy	1980	Rock	NS	32	6.5	0.216	33.06
Marmara	Turkey	1999	Rock	EW	11	7.4	0.227	54.28
Northridge	USA	1994	Rock	360	36.7(d_c)	6.7	0.233	7.46
Friuli	Italy	1976	Rock	EW	27	6.3	0.316	32.63
Campano-Luc.	Italy	1980	Rock	EW	32	6.5	0.323	55.36
Tabas	Iran	1978	Rock	N80W	11	6.4(M_L)	0.338	17.68
Friuli	Italy	1976	Rock	NS	27	6.3	0.357	20.62
Tabas	Iran	1978	Rock	N10E	11	6.4(M_L)	0.385	24.58
Marmara	Turkey	1999	Rock	EW	40	7.4	0.407	79.80
Loma Prieta	USA	1989	Rock	0	2.8(d_c)	7	0.435	31.91
Loma Prieta	USA	1989	Rock	90	2.8(d_c)	7	0.442	33.84
North P. Spr.	USA	1986	USGS(A)	180	7.3(d_c)	6.2	0.492	34.72
North P. Spr.	USA	1986	USGS(A)	270	7.3(d_c)	6.2	0.612	31.48
Morgan Hill	USA	1984	Rock	195	1.5(d_c)	6.1	0.711	51.64
Umbro	Italy	1997	Rock	NS	11	6	0.711	27.61
Umbro	Italy	1997	Rock	EW	11	6	0.760	29.86
Cape Mend.	USA	1992	Rock	90	15.5(d_c)	7	1.039	40.52
Morgan Hill	USA	1984	Rock	285	1.5(d_c)	6.1	1.298	80.79
Cape Mend.	USA	1992	Rock	0	15.5(d_c)	7	1.497	126.12

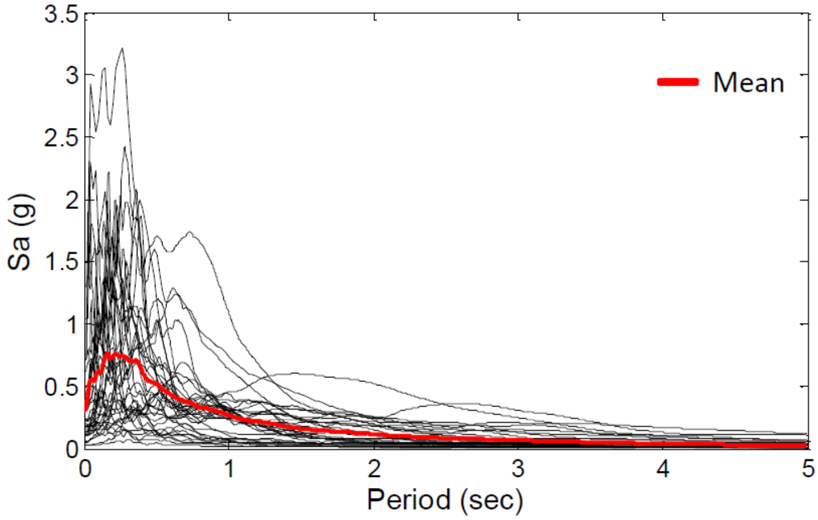

Fig. 3 Pseudo acceleration spectrum of ground motion data set

the dam height, downstream slope, reservoir condition, concrete strength and E_f/E_c) resulted in 120 different cases, which were analyzed for 37 different ground motion records. The total number of conducted analyses was 4440 for the analyses using the EM.

2.3 Earthquake induced stresses

The magnitude of maximum principal tensile stresses (σ_{max}^{u}) at the upstream toe of the concrete dam section during earthquakes is one of the most important engineering demand parameter for the selection of dam size. An appropriate concrete tensile strength should be selected based on stress demand to select an economical and safe dam section. Detailed and accurate response history analysis procedures at an early stage of design may not be possible; hence, beam analogy based procedures are usually employed in the rigid block stability design. Due to the flexibility of dam body and foundation rock, such stress estimations are not accurate. Hence, the earthquake induced stresses on the dam base obtained from the EM analyses results were examined in detail in this section.

Maximum principal tensile stress values at the upstream toe excluding the static (hydrostatic and dam weight) tensile stresses (σ_{max}^{u}) at the dam base obtained by using EM are presented in Fig. 4. Results are shown for different dam heights (H), and they were categorized in three PGA intervals namely, PGA < 0.2g, 0.2g < PGA < 0.4g and PGA > 0.4g separately. Horizontal axes in Fig. 4 were arranged free of scale and actual PGA levels were given as a dashed line. Plots show the stress values and the PGA of the ground motions for different reservoir conditions. For the 50 m high dam, the mean of σ_{max}^{u} values obtained from 37 dynamic analyses were identified as 2.29 MPa and 2.95 MPa for the empty and full reservoir cases, respectively. For the 100 m (150 m) dam section, these values were found as 3.57 MPa (4.49 MPa), 5.47 MPa (6.16 MPa), respectively. These results show that addition of the hydrodynamic effects may increase the average σ_{max}^{u} values by a factor of 1.25 to 1.5. The same condition was observed for individual results of ground motion sets. The scatter in the plots is higher for the full reservoir compared to empty reservoir

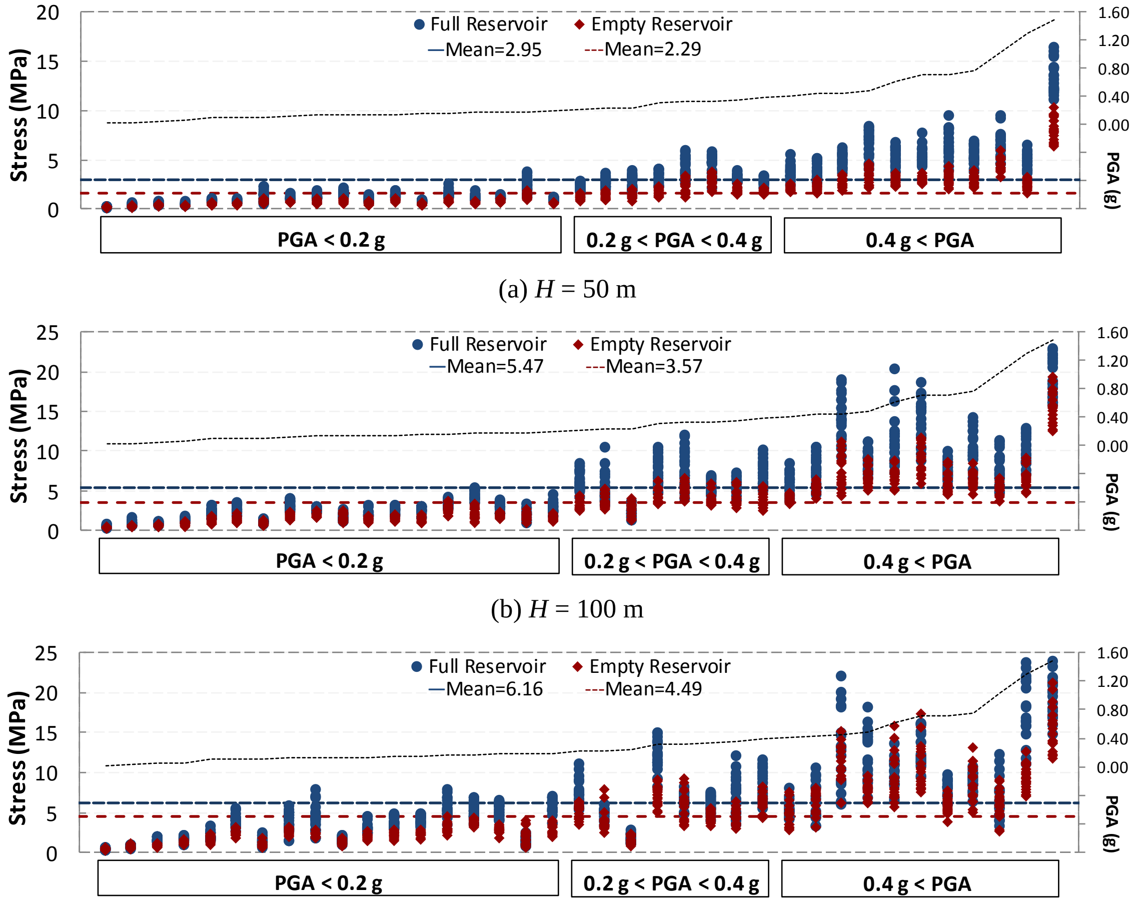

(a) H = 50 m

(b) H = 100 m

(c) H = 150 m

Fig. 4 Maximum principal stress (σ^u_{max}) distributions with varying ground motions

cases. It can be also observed that σ^u_{max} tended to increase with increasing dam height under the influence of the same ground motion. Moreover, ground motions with lower PGAs (PGA < 0.2g) could impose high σ^u_{max} demands on 150 m high dams. This shows that ground motion variability is more important for high dams compared to lower ones.

The effect of examined parameters on σ^u_{max} values was individually studied in Fig. 5. Both empty and full reservoir cases were employed in the figure. Average of σ^u_{max} obtained from 37 response history analysis results for each dam were used for this purpose. According to Fig. 5(a), σ^u_{max} increased with increasing S regardless of H or PGA. For small E_f/E_c values, the effect of S on σ^u_{max} was more influential. The effect of E_c (Fig. 5(b)) did not cause a significant difference for low height dams as well as the ground motions in PGA < 0.2g range. However variation in E_c while keeping E_f/E_c constant may be important for high dams located on softer foundation rock in a region of high seismic hazard. According to Fig. 5(b), σ^u_{max} increases with decreasing E_c values for high dams. The effect of E_f/E_c on σ^u_{max} is found to be one of the most important parameter affecting the σ^u_{max} values. For low height dams, E_f/E_c ratio was less influential on the average

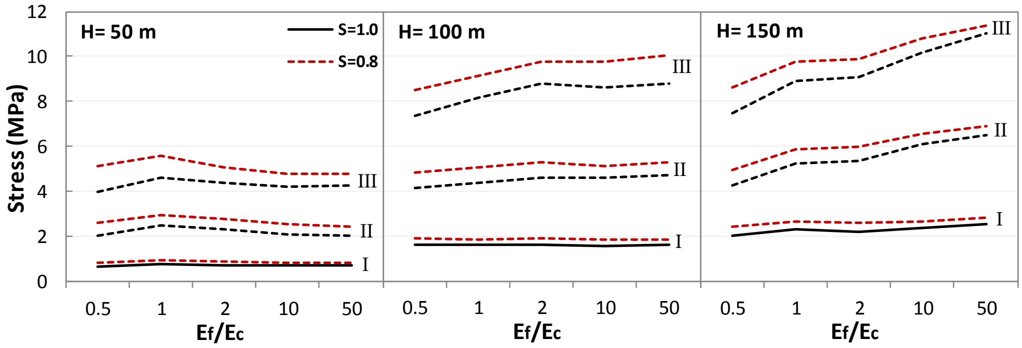

(a) Downstream slope (*S*)

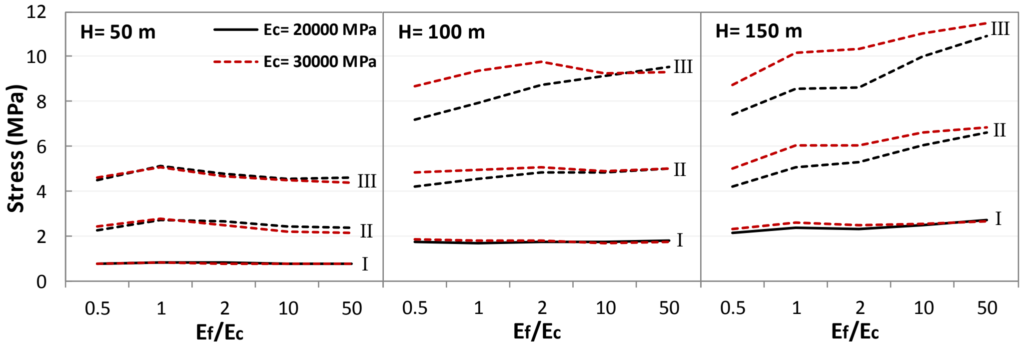

(b) Modulus of elasticity of concrete (E_c)

I: PGA < 0.2 g, II: 0.2 g < PGA < 0.4 g, 0.4 g < PGA

Fig. 5 The effect of parameters on σ_{max}^{u}

Table 2 Coefficients of base stress distribution equation

E_f/E_c	C_1	C_2	C_3	C_4	C_5
0.5	17.88	-38.54	29.27	-8.96	1.00
2	9.91	-24.60	21.77	7.69	1.00
50	3.77	-13.33	14.85	-6.13	1.00

σ_{max}^{u} values. However, for higher dams, σ_{max}^{u} might increase significantly with increasing E_f/E_c, especially for high range of PGA.

The distribution of principal tensile stresses is also important when deciding the critically stressed region under earthquakes. For this purpose, the envelope of principal stress demands (σ_{max}) at the dam base were extracted and plotted by normalizing the dam base with the dam base length (L_b) and stresses with the maximum values as shown in Fig. 6. Both empty and full reservoir cases were employed in the figure. The analysis results revealed that ground motion variability, reservoir condition, *S*, E_c and *H* had negligible effects on stress distribution along the dam base. All the cases related with these parameters were included in stress distribution prediction equation. The main parameter that affected the dam base maximum principal stress envelope distribution was E_f/E_c. In all cases, the maximum principal tensile stresses decreased to 20 percent of their

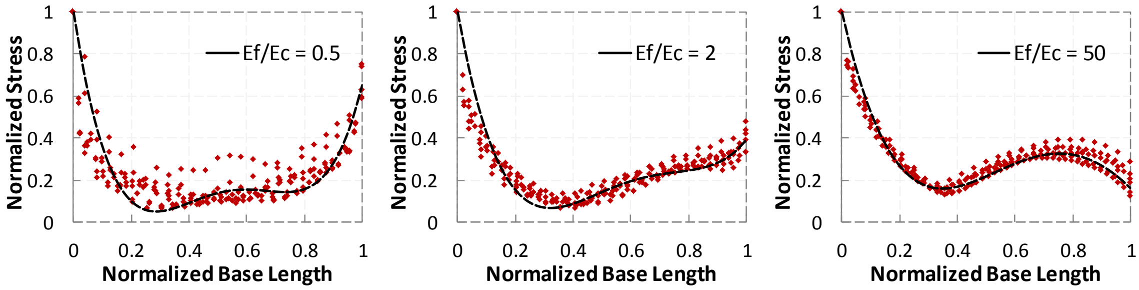

(a) E_f/E_c = 0.5 (b) E_f/E_c = 2 (c) E_f/E_c = 50

Fig. 6 Base stress distributions

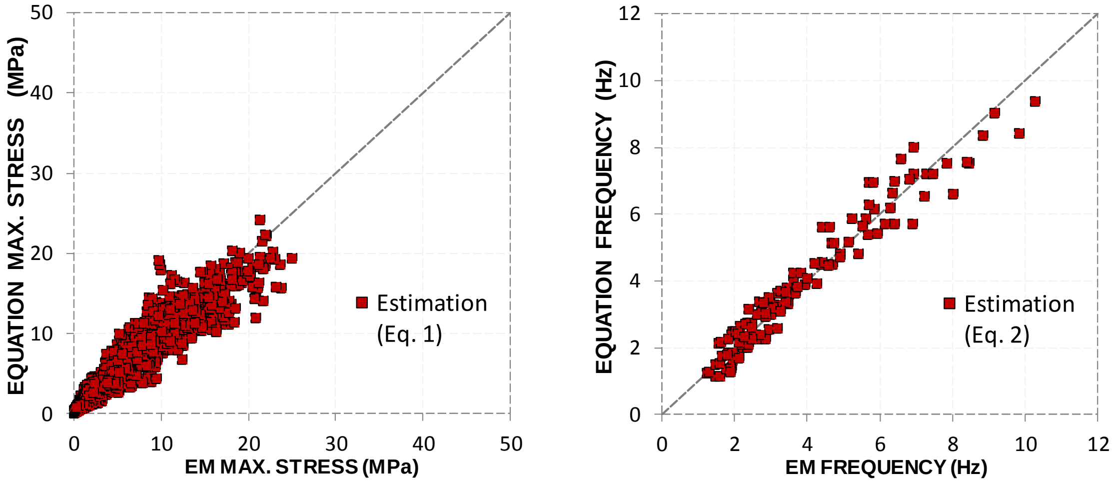

(a) Comparison of σ^u_{max} for EM and Eq. (1) (b) Comparison of F_1 for EM and Eq. (2)

Fig. 7 Accuracy of Eqs. (1) and (2)

maximum values at a distance of $0.2L_b$ from the upstream toe approximately in a linear manner. It is also interesting to note that results in Fig. 6 can be conveniently expressed in the form of a fourth order polynomial, $\frac{\sigma_{max}(x)}{\sigma^u_{max}} = C_1(x/L_b)^4 + C_2(x/L_b)^3 + C_3(x/L_b)^2 + C_4(x/L_b)^4 + C_5$ where x is the distance measured from the upstream toe of the dam base. Constants C_1 to C_5 are given in Table 2 for different E_f/E_c values. The ability of these functions to approximate the σ_{max} distribution is shown in Fig. 6.

The σ^u_{max} values obtained from the numerical simulations using EM was employed in a regression analysis and a stress prediction equation was developed. All important parameters that influence the stress values, namely R (0 for empty, 1 for full), E_f/E_c (E_f/E_c=50 for fixed case), S, H and the spectral acceleration calculated for the fundamental mode of the dam on flexible foundation, S_{a1} (in g) were included in the prediction equation below:

$$\sigma^u_{max} = \left[-5.72 * S + (1.035 + 0.32 * R) * \sqrt{H} - 0.004 * E_f/E_c\right] * {S_{a1}}^{0.9} \tag{1}$$

In order to estimate the spectral accelerations, fundamental frequency of the dam is needed. For this purpose, dam models were analyzed under pulse type loading and the fundamental frequency was extracted for each model by using the frequency amplitude response curves. Based on fundamental frequency results following empirical equation was obtained:

$$F_1 = 78 * E_c H^{-1.55} + 1.77 * (E_f/E_c)^{0.24} - 0.045 * E_c R - 0.25 * \frac{H * E_f/E_c}{1000 * S^2} \tag{2}$$

Above, F_1 represents the first mode frequency (in Hz), E_c modulus of elasticity of concrete (in GPa). Rest of the abbreviations is explained above. The coefficients of determination (R^2) for Eq. (1) and Eq. (2) were found as 0.925 and 0.95, respectively. In Fig. 7(a), the stresses calculated by Eq. (1) are compared with EM results. It can be observed that dynamic stress prediction equations reasonably agree and can be used as a quick estimate of maximum principal stress expected due to earthquakes. Comparisons of the fundamental frequencies estimated by using Eq. (2) and the EM are given in Fig. 7(b). The proposed equation is sufficiently accurate for engineering purposes.

3. Effective damping

3.1 Incompressible fluid massless foundation models (IFMFMs)

"Incompressible Fluid Massless Foundation Model, IFMFM" (Fig. 1(b)) utilizes the added mass approach to model the hydrodynamic forces (Westergaard 1933) along with the massless foundation rock model as proposed by USACE (1995). This modeling approach has many advantages such as allowing existing software to be utilized, ease of handling material nonlinearities in the time domain and allowing first mode static analysis or response spectrum analysis in the absence of ground motion sets. Unfortunately IFMFM may provide significantly different results, when compared to EM results as demonstrated below. In the IFMFM, foundation rock is considered as a massless finite medium while stiffness contribution is taken into account with finite elements extending in a region of at least two times L_B extending all directions. In this way the wave speed is infinity and the input motion can instantaneously reach the dam without any dynamic interaction. Massless foundation models have been commonly employed in the design and evaluation many dams in past studies (e.g., USACE 2003, Chuhan *et al.* 2009 and Leger *et al.* 1989). A critical issue while conducting dynamic analysis using IFMFM is the selection of damping. In order to consider the effects of radiation damping, Fenves and (1986) proposed Eq. 3 derived based on the results of simplified dam analysis.

$$\xi = \frac{1}{R_r R_f^3} \xi_1 + \xi_f + \xi_r \tag{3}$$

Above, ζ_1 represents structural damping, ζ_f represents damping due to dam-foundation interaction and ζ_r represents damping due to reservoir-dam interaction. R_r and R_f accounts for the effect of reservoir and flexible foundation, respectively. Eq. (3) is suggested by USACE (1995) for use along with IFMFMs in seismic analysis of dams. Results presented in the next section were employed by using the IFMFM with effective damping ratios calculated by Eq. (3). The effective damping ratios were adjusted to fit the first and third fundamental frequencies of the dam sections.

3.2 EM versus IFMFM stress results

Maximum principal tensile stress (σ^u_{max}) demands at the dam upstream toe obtained from EM and IFMFM were compared. The results were used to identify the stress errors (i.e., (σ^u_{max} from EM $-$ σ^u_{max} from IFMFM)/σ^u_{max} from EM) obtained from IFMFM for different dam models and ground motions. The identified errors along with the examined parameters are plotted in Fig. 8. Summary of all stress comparisons are shown in Fig. 9.

Modeling the hydrodynamic effects with the added mass along with the massless foundation approach resulted in significant errors irrespective of the dam geometry. For empty reservoir cases, errors were between -60 to 10 percent. The errors were larger and more scattered for the full reservoir conditions compared to the empty reservoir cases showing the additional inaccuracy of the added mass modeling. For the full reservoir conditions, absolute errors tended to increase up to 100%, 130% and 150% for 50 m, 100 m and 150 m dam height. The errors usually tended to increase with decreasing E_f/E_c ratios. The variation of E_c (20000 versus 30000 MPa) did not result in a significant difference on estimated errors. The effect of S seemed to be important on the magnitude of errors unless the foundation was rigid.

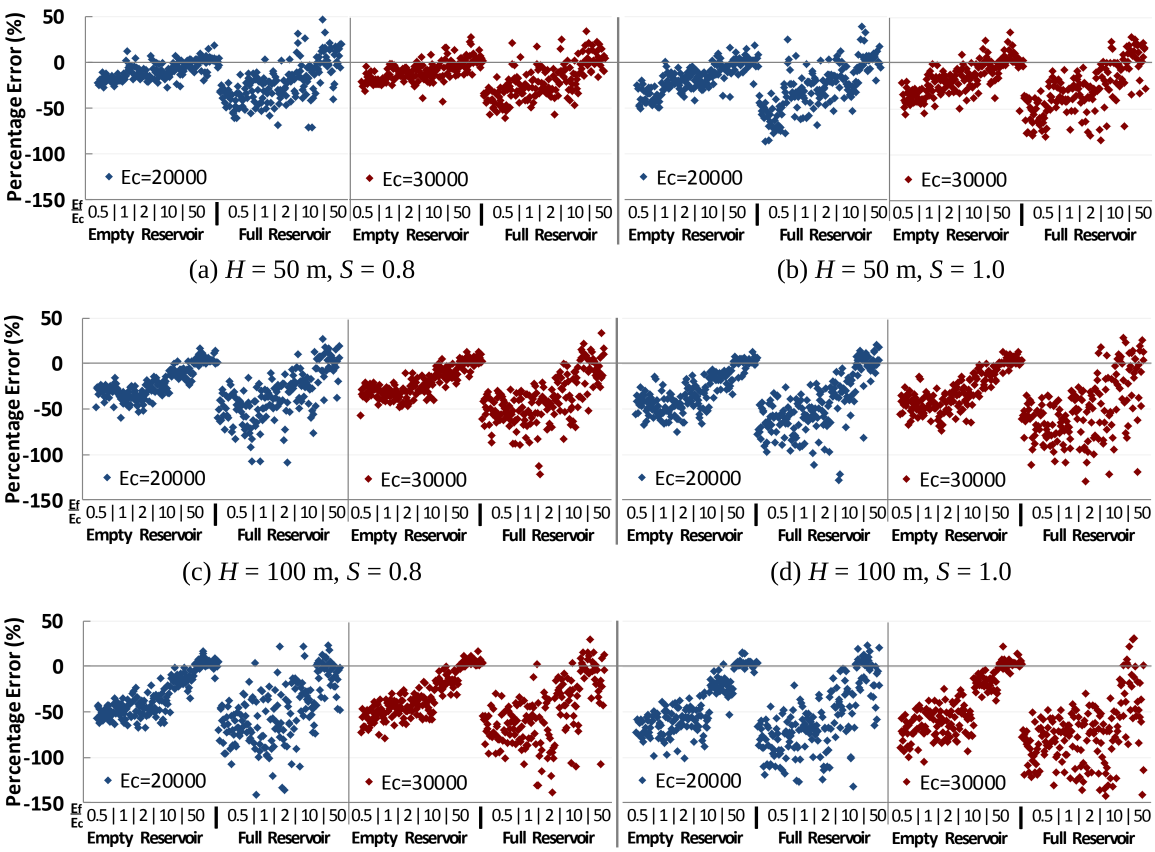

(a) H = 50 m, S = 0.8 (b) H = 50 m, S = 1.0

(c) H = 100 m, S = 0.8 (d) H = 100 m, S = 1.0

(e) H = 150 m, S = 0.8 (f) H = 150 m, S = 1.0

Fig. 8 Maximum stress errors (%) for dams

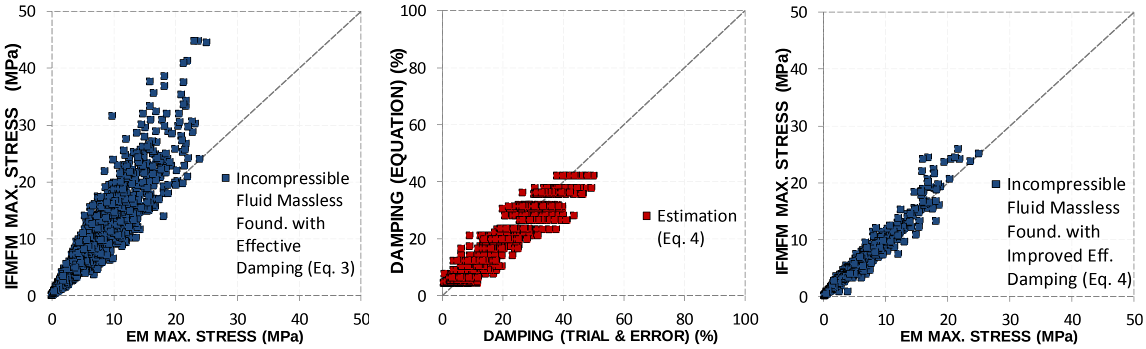

(a) IFMFM stresses with Eq. (3) (b) Estimated damping ratios (%) (c) IFMFM stresses with Eq. (4)

Fig. 9 Comparisons of EM and IFMFM stresses

The sign of the relative errors may also shed light whether the IFMFM (along with simplified damping ratios obtained by Eq. (3)) result in safe (higher than those obtained by using EM) or unsafe estimations (lower than those obtained by using EM). Safety is thought in the design sense whether the engineer overpredicts (safe) or underpredicts (unsafe) the "exact" stresses. According to the results, the main parameter that dictated the safety was E_f/E_c. If this ratio approached to the fixed base case (i.e E_f/E_c=50), the number of having unsafe σ^u_{max} values tended to increase. Conversely, as the foundation rock was softer, stress errors usually grew to large values. Interestingly, E_c and S were not correlated with the sign of the errors. Although increasing H caused an increase in the stress errors; it usually provided safe side estimations. For 50, 100 and 150 m high dams, the percentage for number of analyses that can be labeled as unsafe were 17, 13 and 12, respectively. Significant over prediction of σ^u_{max} can be easily visualized in Fig. 9(a) considering all the data points.

3.3 Improved effective damping

Aforementioned results revealed that IFMF analysis along with modified damping ratios (Fenves and Chopra 1986) provide significant overprediction of σ^u_{max} (up to 150 % in some cases). For preliminary design purposes this situation can be considered as acceptable. However, such models, when used in nonlinear analysis may provide a false picture of the expected damage due to improper estimations of crack initiation. The over simplifications regarding fluid compressibility, frequency dependent nature of foundation stiffness, radiation damping, numerical errors due to time integration, conceptual differences between hysteretic and Rayleigh damping are the likely sources of these errors. One practical way of fixing such high stress errors is using higher damping ratios. This requires finding effective damping ratios that would provide similar σ^u_{max} for IFMFM and EM approaches.

New effective damping ratios were obtained by using an error minimization technique. Damping ratios of the IFMFM was changed until the square root of sum of σ^u_{max} error squares were minimized. For each case, an effective damping ratio was found by employing a trial & error process (Fig. 10). The iterative process was stopped when the σ^u_{max} error between the EM and IFMFM was less than 5 %.

Earlier results in this study show that E_c had negligible effect on σ^u_{max} errors. Moreover, it was decided to compute the effective damping values only for the operation condition corresponding to the full reservoir case. As a result, the effective damping ratios were determined for: H = 50 m, 100 m, 150 m; E_f/E_c = 0.5, 1, 2, 10, 50 and S = 0.8, 1.0. The computed effective damping ratios as a function of H and $1/(E_f/E_c)$ are given in Fig. 11. As can be seen in the figure, effective damping ratios are proportional to $1/(E_f/E_c)$ ratios. To emphasize the correlation of $1/(E_f/E_c)$ values with damping ratios, simple linear trends are also shown. It can also be observed that the increase of S from 0.8 to 1.0 may slightly affect the lower boundaries requiring higher damping ratios.

The effective damping values obtained for each dam section and material properties were averaged for the 37 response history analyses. Results are tabulated in Table 3. It can be stated that, regardless of the E_f/E_c, it is necessary to assign higher effective damping for higher H or S values. Similarly, increasing $1/(E_f/E_c)$ require the use of higher damping ratio demands. In addition,

Fig. 10 Damping ratio identification process

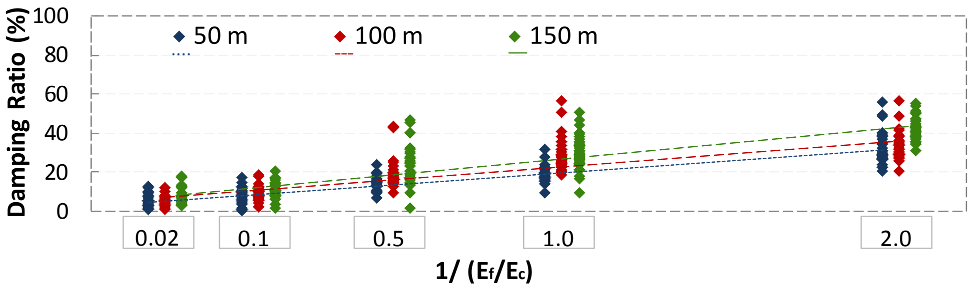

(a) S = 0.8

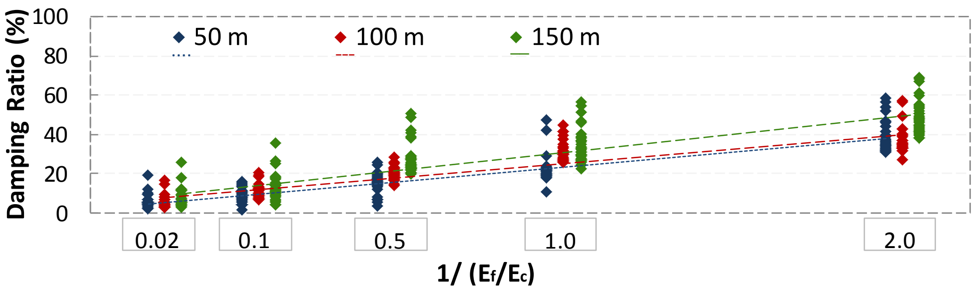

(b) S = 1.0

Fig. 11 Damping ratios (%) for full reservoir and E_c = 20000 MPa

Table 3 Average damping ratios (%) for full reservoir and E_c=20000 MPa

		1/(E_f/E_c)				
	Dam Height (m)	0.02 (Fixed)	0.1	0.5	1	2
S= 0.8	50	4.8	7.1	13.5	18.4	30.8
	100	5.1	8.6	18.4	28.5	32.2
	150	6.8	10.6	22.6	29.7	41.6
S= 1.0	50	5.5	8.3	14.8	21.9	37.8
	100	5.3	10.6	20.1	31.1	36.5
	150	7.2	12.4	27.2	33.5	48.1

effective damping ratios deviate from the assigned material damping in the EM only by a small amount for E_f/E_c=50.

Employing the results above, a nonlinear regression analysis was conducted to propose an equation for effective damping ratios. It should be noted that the provided equation is applicable for the dam sections with 2-dimensional numerical models and utilization of reservoir-dam and foundation-dam interactions with added masses and massless foundation methods, respectively. The proposed equation is as follows:

$$D = \left[-0.007 + \frac{0.65}{H} + 0.005 * \left(E_c/E_f\right)^{F_1} + (0.001 * H + 0.16 * S) * \left(E_c/E_f\right)^{0.4}\right] * 100 \tag{4}$$

In the above equation, D represents the effective damping ratio (%), F_1 represents the first mode frequency (in Hz) that can be calculated by the Eq. (2). It is interesting to note that the effect of ground motion variability was not included as its use through PGA or S_{a1} did not lead to an improvement. In Fig. 9(b), the effective damping ratio estimations of Eq. (4) are compared with the ones obtained from trial & error process. In order to demonstrate the ability of Eq. (4) in estimating σ_{max}^{u} employing the IFMFM, analyses were repeated with the new damping values obtained by using Eq. (4). Comparisons of σ_{max}^{u} employing IFMFM with effective damping from Eq. (4) and using the EM are shown in Fig. 9(c). It can be observed that σ_{max}^{u} estimations are in good agreement with the EM results and the improvement of σ_{max}^{u} estimations upon using Eq. (4) instead of Eq. (3) is remarkable (Fig. 9(a) versus Fig. 9(c)).

The new damping values improve the accuracy of the analysis results and provide nearly uniform error bounds as shown in Fig. 12. However, it can be argued that the proposed damping values may not guarantee safe designs as some of the data lie on the unsafe side. For that reason, a stress magnification factor can be applied to the principal tensile stresses that are determined by the IFMFM. In this way, the use of the proposed damping values can ensure safe designs with an acceptable error margin. Multiplying the maximum tensile stresses obtained with IFMFM (employing the new damping values) by 1.15 guarantees that 90% of the results are on the safe side (Fig. 13).

4. Conclusions

By conducting 4440 analyses with the exact (Fenves and Chopra 1984) and simplified methods, dam base stresses and effective damping of concrete gravity dams were investigated. The

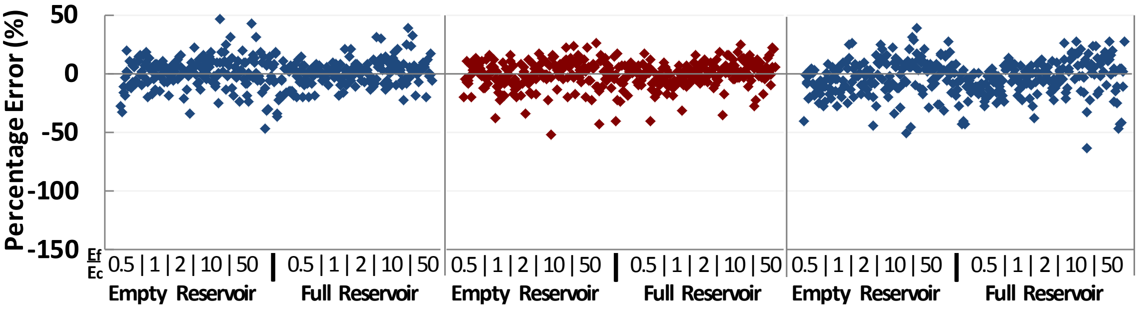

(a) H = 50 m (b) H = 100 m (c) H = 150 m

Fig. 12 The errors of maximum principal stress with improved effective damping

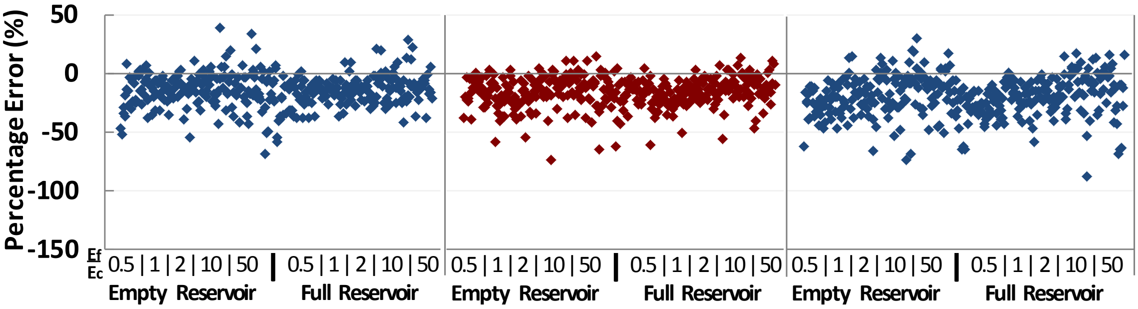

(a) H = 50 m (b) H = 100 m (c) H = 150 m

Fig. 13 The errors of maximum principal stress with magnification factor

maximum principal tensile stress (σ^{u}_{max}) at the dam upstream toe and its distribution at the dam base were studied. Results showed that the tensile stress distribution at the base was strongly correlated with the E_f/E_c ratio. Higher dams with full reservoir were usually exposed to higher principal tensile stress demands and the effect of E_f/E_c on σ^{u}_{max} was found to be more important. A simple prediction equation for σ^{u}_{max} was proposed as a function of R, E_f/E_c, S, H and S_{a1}. Accuracy of stress estimations using the IFMFM, which is a practical and frequently preferred analysis method for reservoir-foundation-structure interaction problems, was critically evaluated. Results showed that the method along with the Eq. (3) led to significant errors in stress estimations. The influential variables on errors were dam height, reservoir condition and E_f/E_c. The boundaries of the stress errors usually showed larger scatter for the full reservoir condition due to the added inaccuracy from the added mass approach. IFMFM usually ensured safe side stress estimations except when the E_f/E_c ratio approaches to the fixed base case. In order to minimize the stress errors caused by IFMFM, the damping ratios were adjusted by using an error minimization technique. The results showed that higher dams with low E_f/E_c ratio required significantly high damping ratios. The E_f/E_c ratio was found to be the most important variable for the damping ratios and almost a linear relationship was observed between the inverse of E_f/E_c and damping ratios. The effectiveness of the new damping equation was successfully proved by comparing to the earlier numerical tests. However, one should be cautious for the high damping ratios predicted by using

Eq. (4) due to the inability of the two dimensional half space problems in providing an accurate picture of the actual dam site conditions.

References

Arici, Y. and Binici, B. (2011), "Seismic safety assessment of Andiraz dam", BAP Report No. 2010-03-03-1-00-20, Civil Engineering Department, METU, Ankara, TR.

Bhattacharjee, S.S. and Leger, P. (1995), "Fracture response of gravity dams due to rise of reservoir elevation", *J. Struct. Eng.*, **121**(9), 1298-1305.

Bougacha, S., Roësset, J. and Tassoulas, J. (1993), "Dynamic stiffness of foundations on fluid-filled poroelastic stratum", *J. Eng. Mech.*, **119**(8), 1649-1662.

Chopra, A.K. (1966), "Hydrodynamic pressures on dams during earthquakes", Report No. UCB/EERC-66/2-A, Earthquake Engineering Research Center, University of California, Berkeley, CA.

Chuhan, Z., Jianwen, P. and Jinting, W. (2009), "Influence of seismic input mechanisms and radiation damping on Arch dam response", *Soil Dym. Earthq. Eng.*, **29**, 1282-1293.

Dasgupta, G. and Chopra, A.K. (1977), "Dynamic stiffness matrices for homogeneous viscoelastic half-planes", Report No. UCB/EERC-77/26, Earthquake Engineering Research Center, University of California, Berkeley, CA.

Fenves, G. and Chopra, A.K. (1984), "Earthquake analysis and response of concrete gravity dams", Report No. UCB/EERC-84/10, Earthquake Engineering Research Center, University of California, Berkeley, CA.

Fenves, G. and Chopra, A.K. (1984), "EAGD-84: a computer program for earthquake analysis of concrete gravity dams", Report No. UCB/EERC-84/11, Earthquake Engineering Research Center, University of California, Berkeley, CA.

Fenves, G. and Chopra, A.K. (1986), "Simplified analysis for earthquake resistant design of concrete gravity dams", Report No. UCB/EERC-85/10, Earthquake Engineering Research Center, University of California, Berkeley, CA.

Javanmardi, F., Leger, P. and Tinawi, R. (2005), "Seismic water pressure in cracked concrete gravity dams: Experimental study and theoretical modeling", *J. Struct. Eng.- ASCE*, **131**(1), 139-150.

Leger, P. and Boughoufalah, M. (1989), "Earthquake input mechanisms for time-domain analysis of dam-foundation systems", *Eng. Struct.*, **11**, 37-46.

Lotfi, V. and Arabshahi, H. (2008), "Earthquake response of concrete gravity dams including dam–foundation interface nonlinearities", *Eng. Struct.*, **30**, 3065-3073.

Lotfi, V., Roesset, J.M. and Tassoulas, J.L. (1987), "A technique for the analysis of the response of dams to earthquakes", *Earthq. Eng. Struct. D.*, **15**(4), 463-490.

Mclean, P., Leger, P. and Tinawi, R. (2006), "Post-processing of finite element stress fields using dual kriging based methods for structural analysis of concrete dams", *Finite Elem. Anal. Des.*, **42**, 532-546.

Medina, F., Dominguez, J. and Tassoulas, J. (1990), "Response of dams to earthquakes including effects of sediments", *J. Struct. Eng.*, **116**(11), 3108-3121.

USACE (1995), "Seismic design provisions for roller compacted concrete dams", No. EP-1110-2-12, United States Army Corps of Engineers.

USACE (2003), "Time-history dynamic analysis of concrete hydraulic structures", EM 1110-2-6051, United States Army Corps of Engineers.

Westergaard, H.M. (1933), "Water pressures on dams during earthquakes", *Trans. Am. Soc. Civil Eng.*, **98**, 418-434.

SA